Mineralogical Magazine (2020), **84**, 283–287
doi:10.1180/mgm.2019.69

Article

Koryakite, $NaKMg_2Al_2(SO_4)_6$, a new NASICON-related anhydrous sulfate mineral from Tolbachik volcano, Kamchatka, Russia

Oleg I. Siidra[1,2]*, Evgeny V. Nazarchuk[1], Anatoly N. Zaitsev[3] and Natalia S. Vlasenko[4]

[1]Department of Crystallography, St. Petersburg State University, University Embankment 7/9, 199034 St. Petersburg, Russia; [2]Kola Science Center, Russian Academy of Sciences, Apatity, Murmansk Region, 184200 Russia; [3]Department of Mineralogy, St. Petersburg State University, University Embankment 7/9, 199034 St. Petersburg, Russia; and [4]Geomodel Centre, St. Petersburg State University, University Embankment 7/9, 199034 St. Petersburg, Russia

Abstract

Exhalative mineral assemblages from fumaroles of Tolbachik volcano are very rich in anhydrous sulfate minerals of alkali and transition metals. Koryakite, ideally $NaKMg_2Al_2(SO_4)_6$, was found in the Yadovitaya fumarole of the Second scoria cone of the North Breach of the Great Tolbachik Fissure Eruption (1975–1976), Tolbachik volcano, Kamchatka Peninsula, Russia. Koryakite occurs as a product of fumarolic activity and closely associates with euchlorine and langbeinite. Koryakite is trigonal, $R\bar{3}$, $a = 8.1124(11)$, $c = 22.704(7)$ Å and $V = 1294.0(5)$ Å^3. The chemical composition determined by electron-microprobe analysis is (wt.%): Na_2O 4.27, K_2O 5.85, ZnO 0.31, CaO 0.31, CuO 0.76, MgO 10.15, Al_2O_3 11.47, Fe_2O_3 2.73, SO_3 64.33 and SiO_2 0.13, total 100.31. The empirical formula calculated on the basis of 24 O apfu is $Na_{1.03}K_{0.93}(Mg_{1.89}Cu_{0.07}Ca_{0.04}Zn_{0.03})_{\Sigma2.03}(Al_{1.68}Fe^{3+}_{0.26})_{\Sigma1.94}(S_{6.02}Si_{0.02})_{\Sigma6.04}O_{24}$. No natural or synthetic chemical analogues of koryakite are known to date. The topology of the $[M^{2+}_2M^{3+}_2(SO_4)_6]^{2-}$ heteropolyhedral framework in koryakite is very similar to the one in millosevichite, $Al_2(SO_4)_3$ and mikasaite, $Fe^{3+}_2(SO_4)_3$. Replacement of part of the trivalent cations in the $[M^{3+}_2(SO_4)_3]^0$ framework by divalent cations gives the framework a negative charge for koryakite and allows the incorporation of the alkali species in the channels. This structural mechanism is reminiscent of the concept of stuffed derivative structures. Koryakite is also structurally related to synthetic $NaMgFe^{3+}(SO_4)_3$ and to the broader family of NASICON-related phases.

Keywords: koryakite, new minerals, sulfates, framework structures, $Al_2(SO_4)_3$, $Fe_2(SO_4)_3$, stuffed derivative structures, NASICON, Tolbachik volcano

(Received 29 July 2019; accepted 24 October 2019; Accepted Manuscript published online: 4 November 2019; Associate Editor: Koichi Momma)

Introduction

Anhydrous sulfates of alkali and/or transition metals are very sensitive to moist air. Due to this fact, the number of described anhydrous sulfate mineral species with transition and alkali metals is limited. A number of these minerals are known from active volcanic fumaroles with oxidising environments. Exhalative mineral assemblages from fumaroles of the First and Second scoria cones, Great Fissure Tolbachik eruption 1975–76 (Fedotov and Markhinin, 1983) are very rich in anhydrous sulfate minerals of alkali and transition metals (mostly Cu^{2+}) (Vergasova and Filatov, 2012).

Herein we report on the chemical composition, structure and properties of koryakite (Cyrillic: корякит), $NaKMg_2Al_2(SO_4)_6$. The mineral is named for the Koryaks, an ethnic group who are the original inhabitants living on the Kamchatka peninsula. Both the mineral and the mineral name were approved by the Commission on New Minerals, Nomenclature and Classification of the International Mineralogical Association (IMA2018-013, Nazarchuk *et al.*, 2018). Type material is deposited at the Mineralogical Museum, St. Petersburg State University, St. Petersburg, Russia (catalogue no. 1/19688).

Occurrence and association

Koryakite occurs as a product of fumarolic activity. It was found in June 2016 in the Yadovitaya fumarole, Second scoria cone, North Breach, Great Fissure eruption, Tolbachik volcano, Kamchatka, Russia (55°49′59″N, 160°19′59″E). The Second Scoria Cone is located ∼18 km SSW of the active shield volcano Ploskiy Tolbachik (Fedotov and Markhinin, 1983). Koryakite closely associates with euchlorine (Fig. 1) and langbeinite. Koryakite is a fumarolic mineral that is deposited directly from volcanic gas emissions as a sublimate. The temperature of gases at the sampling location was ∼300°C. All the recovered samples were packed immediately and isolated when collected to avoid any contact with the external atmosphere.

Physical properties

Koryakite is colourless (Fig. 1), has a white streak and vitreous lustre. The mineral is brittle with uneven fracture. Cleavage or parting has not been observed. Hardness corresponds to 2–3 on the Mohs' scale. The density could not be measured due to the lack of an appropriate sample, but it has been calculated as

---

*__Author for correspondence:__ Oleg I. Siidra, Email: o.siidra@spbu.ru

Cite this article: Siidra O.I., Nazarchuk E.V., Zaitsev A.N. and Vlasenko N.S. (2020) Koryakite, $NaKMg_2Al_2(SO_4)_6$, a new NASICON-related anhydrous sulfate mineral from Tolbachik volcano, Kamchatka, Russia. *Mineralogical Magazine* **84**, 283–287. https://doi.org/10.1180/mgm.2019.69

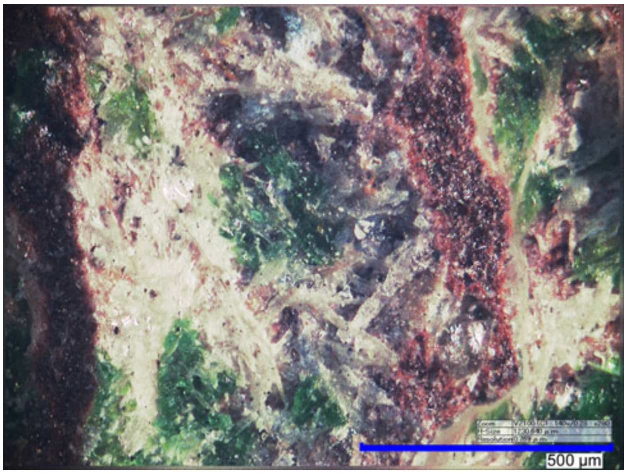

Fig. 1. Abundant elongated white transparent crystals of koryakite in association with green euchlorine in the voids of basaltic scoria.

Table 1. Compositional data (wt.%) for koryakite.

Constituent	Mean	Range	S.D.	Probe standard
Na_2O	4.27	3.95–4.46	0.17	NaCl
K_2O	5.85	5.65–5.98	0.13	KCl
ZnO	0.31	0.22–0.40	0.07	Zn
CaO	0.31	0.25–0.47	0.07	$Ca(SO_4)$
CuO	0.76	0.60–0.96	0.10	Cu
MgO	10.15	9.81–10.47	0.22	MgO
Al_2O_3	11.47	11.21–11.94	0.27	Al_2O_3
Fe_2O_3	2.73	2.23–3.26	0.31	FeS_2
SO_3	64.33	63.18–65.10	0.62	$Ca(SO_4)$
SiO_2	0.13	0.11–0.19	0.03	SiO_2
Total	100.31			

S.D. – standard deviation

2.892 g cm^{-3} using structural data and the empirical formula. No fluorescence is detected.

Koryakite is optically uniaxial (–), ω = 1.546(2) and ε = 1.535(2). Microscopically, it is colourless and non-pleochroic. Compatibility [1 – (K_P/K_C) = 0.030] is excellent (Mandarino, 1981).

Chemical composition

One crystal (110 µm × 55 µm in size) was mounted in epoxy resin and polished with oil suspension. Compositional data from energy-dispersive spectroscopy (EDS) analyses ($N = 8$) (Table 1) were obtained using a Hitachi S-3400N scanning electron microscope equipped with an Oxford Instruments X-Max 20 Energy Dispersive Spectrometer. The electron beam accelerating voltage was 20 kV and the current 1.8 nA; a defocused beam (10 µm spot size) was used and the X-ray acquisition time was 30 s. The mineral is stable under the electron beam; no surface damage was observed after analyses.

The empirical formula calculated on the basis of 24 O atoms per formula unit (apfu) is $Na_{1.03}K_{0.93}(Mg_{1.89}Cu_{0.07}Ca_{0.04}Zn_{0.03})_{\Sigma 2.03}(Al_{1.68}Fe^{3+}_{0.26})_{\Sigma 1.94}(S_{6.02}Si_{0.02})_{\Sigma 6.04}O_{24}$. The simplified formula is $NaKMg_2Al_2(SO_4)_6$, which requires Na_2O 4.18, K_2O 6.36, MgO 10.88, Al_2O_3 13.76, SO_3 64.83, total 100.00 (wt.%).

Koryakite is soluble in warm H_2O.

Table 2. Powder X-ray diffraction data (*d* in Å) for koryakite.

I_{meas}	d_{calc}	d_{meas}	*h*	*k*	*l*
5	6.7116	6.7422	1	0	1
10	**5.9740**	**5.9359**	**1**	**0**	$\bar{2}$
2	4.4151	4.3943	1	0	4
1	4.0562	4.0673	1	1	0
5	3.7840	3.7937	0	0	6
55	**3.5751**	**3.5850**	**1**	**1**	**3**
4	3.3558	3.3688	2	0	2
4	2.9870	2.9819	2	0	$\bar{4}$
100	**2.7669**	**2.7632**	**1**	**1**	**6**
7	2.6374	2.6334	2	1	1
22	**2.3418**	**2.3397**	**3**	**0**	**0**
2	2.2372	2.2363	3	0	3
2	2.2076	2.2131	2	0	8
12	**2.1604**	**2.1582**	**1**	**0**	**10**
7	2.1422	2.1405	1	1	9
9	1.9913	1.9906	3	0	6
5	1.8920	1.8900	0	0	12
1	1.8430	1.8411	1	3	4
30	**1.7875**	**1.7890**	**2**	**2**	**6**
3	1.6779	1.6782	4	0	4
3	1.6703	1.6688	1	3	7
6	1.6064	1.6078	3	1	8
1	1.5806	1.5799	2	2	9
1	1.5802	1.5811	1	0	$\overline{14}$

The strongest lines are given in bold.

X-ray crystallography

Experiment

Powder X-ray diffraction data were collected using a Rigaku R-AXIS Rapid II single-crystal diffractometer equipped with cylindrical image plate detector using Debye–Scherrer geometry (Co*K*α radiation, $d = 127.4$ mm). For the powder-diffraction study, a Gandolfi-like motion was used to randomise the sample.

Table 3. Crystallographic data and refinement parameters for koryakite.

Crystal data	
Ideal formula	$NaKMg_2Al_2(SO_4)_6$
Crystal size (mm)	0.30 × 0.30 × 0.03
Crystal system, space group	Trigonal, $R\bar{3}$
Temperature (K)	293
Unit-cell dimensions *a*, *c* (Å)	8.1124(11), 22.704(7)
Unit-cell volume (Å^3)	1294.0(5)
Z	3
Calculated density (g cm^{-3})	2.880
Absorption coefficient (mm^{-1})	1.560
Data collection	
Radiation, wavelength (Å)	Mo*K*α, 0.71073
F(000)	1114
θ range (°)	2.691–30.999
h, *k*, *l* ranges	$-8 \leq h \leq 11$, $-11 \leq k \leq 8$, $-18 \leq l \leq 32$
Total reflections collected	2480
Unique reflections (R_{int})	909 (0.0848)
Unique reflections $F > 4\sigma(F)$	765
Structure refinement	
Refinement method	Full-matrix least-squares on F^2
Weighting coefficients *a*, *b*	0.12920, 0
Data/restraints/parameters	909/0/59
R_1 [$F > 4\sigma(F)$], wR_2 [$F > 4\sigma(F)$]	0.0722, 0.2197
R_1 all, wR_2 all	0.0792, 0.2231
Gof on F^2	1.220
Largest diff. peak and hole (e^- Å^{-3})	2.959, –0.815

Table 4. Bond-valence sums (BVS), coordinates, anisotropic and isotropic displacement parameters (Å) of atoms in koryakite.

Atom	Site	BVS	x	y	z	U_{eq}	U^{11}	U^{22}	U^{33}	U^{23}	U^{13}	U^{12}
K	3*b*	0.93	⅓	⅔	⅙	0.0328(10)	0.0396(16)	0.0396(16)	0.0192(17)	0	0	0.0198(8)
Na	3*a*	0.91	0	0	0	0.0192(14)	0.024(2)	0.024(2)	0.010(3)	0	0	0.0119(11)
*M*1*	6*c*	3.09	⅔	⅓	−0.01135(11)	0.0077(9)	0.0064(10)	0.0064(10)	0.0104(13)	0	0	0.0032(5)
*M*2**	6*c*	2.16	⅔	⅓	0.18547(13)	0.0094(10)	0.0095(13)	0.0095(13)	0.0093(16)	0	0	0.0048(6)
S1	18*f*	6.03	0.3743(2)	0.3382(2)	0.08027(6)	0.0099(4)	0.0120(7)	0.0095(7)	0.0075(6)	0.0004(4)	0.0008(5)	0.0049(5)
O1	18*f*	1.97	0.4717(8)	0.3623(8)	0.1360(2)	0.0203(11)	0.021(3)	0.030(3)	0.012(2)	−0.0002(18)	−0.0036(17)	0.015(2)
O2	18*f*	1.99	0.4468(7)	0.2586(7)	0.0347(2)	0.0172(10)	0.016(2)	0.016(2)	0.020(2)	0.0015(18)	0.0079(18)	0.0089(19)
O3	18*f*	2.04	0.1701(7)	0.2062(7)	0.0860(2)	0.0160(10)	0.012(2)	0.014(2)	0.020(2)	0.0026(16)	0.0033(17)	0.006(2)
O4	18*f*	2.09	0.4090(7)	0.5293(7)	0.06206(19)	0.0151(10)	0.017(2)	0.009(2)	0.020(2)	0.0004(15)	−0.0023(17)	0.0070(19)

*$Al_{0.88(2)}Fe_{0.12(2)}$; **Rounded and fixed in agreement with microprobe data as $Mg_{0.93}Cu_{0.035}Ca_{0.02}Zn_{0.015}$.
Bond-valence sums for mixed *M*1 and *M*2 sites were calculated using parameters for Al–O and Mg–O bonds from Brese and O'Keeffe (1991), respectively.

Table 5. Selected interatomic distances (Å) in koryakite.

K–O4	2.819(5) × 6	*M*2–O1	2.047(5) ×3	S–O1	1.452(5)
K–O1	3.258(5) × 6	*M*2–O3	2.088(5) ×3	S–O3	1.461(5)
		<*M*2–O>	2.068	S–O2	1.488(5)
Na–O3	2.492(5) × 6			S–O4	1.489(5)
Na–O2	3.249(5) × 6	*M*1–O2	1.887(5) ×3	<S–O>	1.472
		*M*1–O4	1.904(5) ×3		
		<*M*1–O>	1.896		

Data (in Å) are given in Table 2. Unit-cell parameters refined from the powder data processed using *osc2xrd* software (Britvin *et al.*, 2017) are as follows: rhombohedral, space group $R\bar{3}$, a = 8.1129(2) Å, c = 22.7064(9) Å, V = 1294.28(8) $Å^3$ and Z = 3.

A transparent platy crystal fragment of koryakite was mounted on a thin glass fibre for X-ray diffraction analysis using a Bruker APEX II DUO X-ray diffractometer with a micro-focus X-ray tube operated with Mo*K*α radiation at 50 kV and 40 mA. The data were integrated and corrected for absorption using a multi-scan type model implemented in the Bruker programs *APEX* and *SADABS* (Bruker-AXS, 2014). More than a hemisphere of X-ray diffraction data was collected. The structure was solved by direct methods and refinement by means of the *SHELX* program (Sheldrick, 2015) in the $R\bar{3}$ space group converged to R_1 = 0.072 (Table 3). The twinning matrix $[0\ \bar{1}\ 0/\ \bar{1}\ 0\ 0/\ 0\ 0\ 1]$ was employed during the crystal-structure refinement. The refined twin ratio of the two components was 0.199(1):0.801(1). The *M*2 site was modelled on an Mg scattering curve (Mg being the major component) and the resulting site occupancy factor of 1.07(2) is supporting the proposed mixed composition for the *M*2 site based on EDS analysis (Table 1). The final model included anisotropic displacement parameters for all atoms. The final atomic coordinates and anisotropic displacement parameters are given in Table 4 and selected interatomic distances in Table 5. Bond-valence sums are given in Table 4. All bond-valence parameters were taken from Brese and O'Keeffe (1991). All of the bond-valence sums are in good agreement with the expected oxidation states for all atoms. Lists of observed and calculated structure factors have been deposited with the Principal Editor of *Mineralogical Magazine* and are available as Supplementary material (see below).

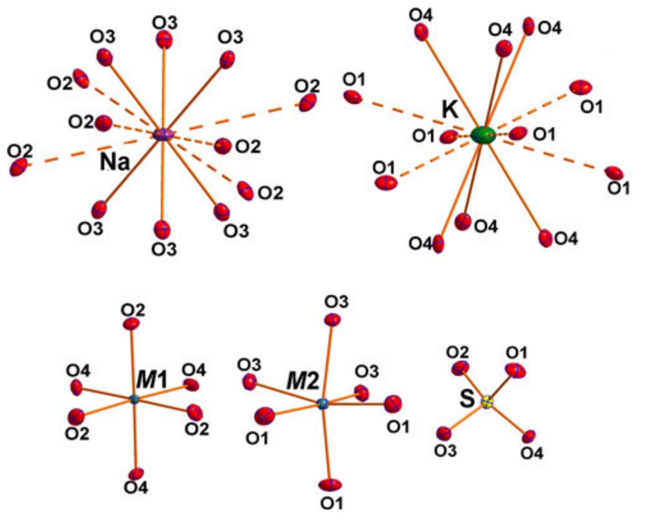

Fig. 2. Coordination polyhedra of cations in the structure of koryakite. Displacement ellipsoids are drawn at 50% probability level.

Crystal structure

The crystal structure of koryakite contains five symmetrically independent cationic sites (Fig. 2, Table 4). K and Na sites are occupied exclusively by K^+ and Na^+ cations, respectively. The K site is symmetrically coordinated by six bonds K–O4 = 2.819(5) Å and by six K–O1 = 3.258(5) Å. This $KO4_6$ polyhedron is a trigonal antiprism. Similar coordination environments are observed for the Na site with six Na–O3 = 2.492(5) Å and six Na–O2 = 3.249(5) Å bonds.

There are two octahedrally coordinated *M* sites. An octahedral *M*1 site is occupied exclusively by Al^{3+} and Fe^{3+} cations. The refined ratio of Al:Fe (Table 4) is close to that obtained by microprobe analysis. The *M*2 site is predominantly occupied by Mg^{2+} cations and its full occupation by various divalent cations was fixed in agreement with microprobe data. M1–O bonds in the $M^{3+}1O_6$ octahedron are shorter than M2–O bonds in $M^{2+}2O_6$ (Table 5). Both of the octahedra are slightly distorted.

One S site is compatible with occupancy by S^{6+} and tetrahedrally coordinated by O anions. The <S–O> distance is 1.472 Å, which is in an excellent agreement with the <S–O> distance of 1.473 Å reported for sulfate minerals by Hawthorne *et al.* (2000).

$M^{3+}1O_6$ and $M^{2+}2O_6$ octahedra are isolated from each other in the structure of koryakite. The SO_4 tetrahedron shares each of its vertices with $M^{3+}1O_6$ and $M^{2+}2O_6$ octahedra and each $M^{3+}1O_6$ and $M^{2+}2O_6$ octahedron is linked to six SO_4 tetrahedra. Thus a three-dimensional $[M^{2+}_2M^{3+}_2(SO_4)_6]^{2-}$ heteropolyhedral framework is formed (Fig. 3*a*). The channels run parallel to [001], where Na^+ and K^+ cations are located (Fig. 3*b*,*c*). The channel walls are lined by sulfate tetrahedra both in the case of Na and

https://doi.org/10.1180/mgm.2019.69

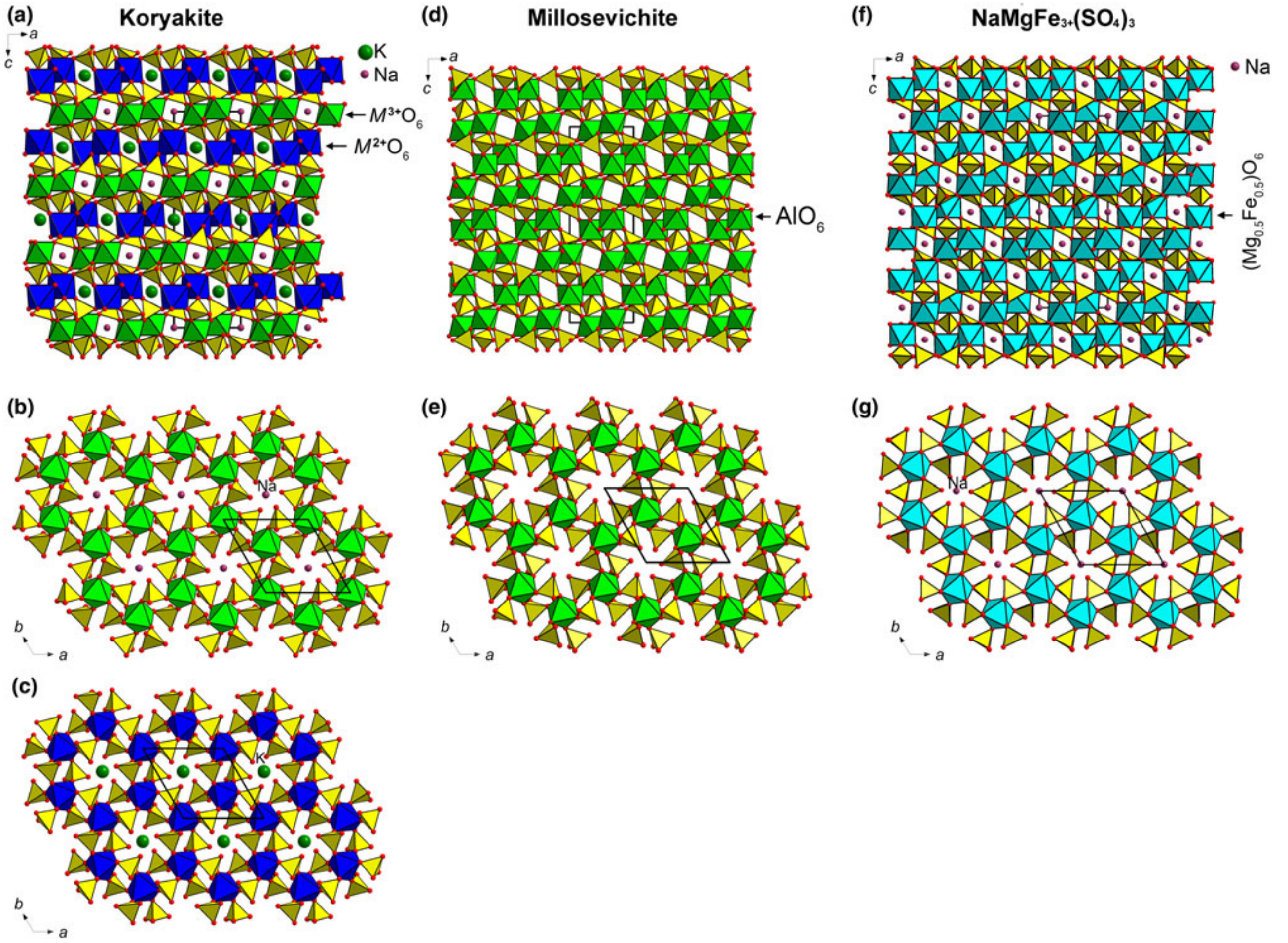

Fig. 3. General projection of the crystal structure of (*a*) koryakite ($M^{3+}1O_6$ = green; $M^{2+}2O_6$ = blue; and SO_4 = yellow) with the channels filled by Na^+ and K^+ cations. The framework can be split into layers (*b*,*c*). The channels are empty in (*d*,*e*) millosevichite $Al_2(SO_4)_3$ (after Dahmen and Gruehn, 1993) (AlO_6 = green) and filled by Na^+ cations in (*f*,*g*) synthetic $NaMgFe^{3+}(SO_4)_3$ (after Slater and Greaves, 1994) ($(Mg_{0.5}Fe^{3+}_{0.5})O_6$ = turquoise).

Table 6. Crystal chemical data of koryakite, millosevichite, mikasaite and synthetic $NaMgFe^{3+}(SO_4)_3$.

Mineral	Koryakite	Millosevichite	Mikasaite	–
Formula	$NaKMg_2Al_2(SO_4)_6$	$Al_2(SO_4)_3$	$Fe^{3+}_2(SO_4)_3$	$NaMgFe^{3+}(SO_4)_3$
Crystal system	Trigonal	Trigonal	Trigonal	Trigonal
Space group	$R\bar{3}$	$R\bar{3}$	$R\bar{3}$	$R\bar{3}$
a (Å)	8.1124(11)	8.0246(4)	8.2362(2)	8.49290(1)
c (Å)	22.704(7)	21.3570(10)	22.1786(10)	21.9749(2)
V (Å^3)	1294.0(5)	1191.02	1302.92	1372.68
Z	3	6	6	6

K. Na^+ cations are segregated in the layers containing the smaller $M^{3+}1O_6$ octahedra (Fig. 3*b*), whereas K^+ cations are segregated in the layers with the relatively larger $M^{2+}2O_6$ octahedra (Fig. 3*c*).

Discussion

No natural or synthetic chemical analogues of koryakite are known to date. The topology of the $[M^{2+}_2M^{3+}_2(SO_4)_6]^{2-}$ framework in koryakite is very similar to that in millosevichite $Al_2(SO_4)_3$ (Dahmen and Gruehn, 1993) (Fig. 3*b*,*d*) and mikasaite $Fe^{3+}_2(SO_4)_3$ (Christidis and Rentzeperis, 1976) (Table 6). Replacement of the part of the trivalent cations in the $[M^{3+}_2(SO_4)_3]^0$ framework (Fig. 3*b*) by divalent cations provides the negative charge and allows the incorporation of the alkali species in the channels, which are empty in millosevichite and mikasaite. This structural mechanism is reminiscent of the concept of stuffed derivative structures first proposed by Buerger (1954). Thus, the distant analogy of observed millosevichite–koryakite structural relationships can be found in silicates, as e.g. nepheline with a crystal structure derived from tridymite (Abbott, 1984). Regardless of the complex substitutions observed in koryakite, its general structural motif and the symmetry remain the same as in a parent $Al_2(SO_4)_3$ crystal structure (Dahmen and Gruehn, 1993).

Koryakite is related structurally to $NaMgFe^{3+}(SO_4)_3$ (Table 6) (Slater and Greaves, 1994) and, as well as this compound, to the broader family of NASICON-related phases (Anantharamulu *et al.*, 2011). The $(Mg_{0.5}Fe^{3+}_{0.5})O_6$ octahedra have a mixed occupancy in $NaMgFe^{3+}(SO_4)_3$ (Fig. 3*f*) and Na^+ cations are located in the channels similar to koryakite.

Acknowledgements. We are grateful to Tonči Balić-Žunić, one anonymous reviewer and Peter Leverett for valuable comments. This work was supported financially by the Russian Science Foundation, grant no. 16-17-10085. Technical support by the SPbSU X-ray Diffraction and Geomodel Resource Centres is gratefully acknowledged.

Supplementary material. To view supplementary material for this article, please visit https://doi.org/10.1180/mgm.2019.69

References

Abbott R.N. (1984) $KAlSiO_4$ stuffed derivatives of tridymite: phase relationships. *American Mineralogist*, **69**, 449–457.

Anantharamulu N., Koteswara Rao K., Rambabu G., Kumar V., Radha V. and Vithal M. (2011) A wide-ranging review on nasicon type materials. *Journal of Materials Science*, **46**, 2821–2837.

Brese N.E. and O'Keeffe M. (1991) Bond-valence parameters for solids. *Acta Crystallographica*, **B47**, 192–197.

Britvin S.N., Dolivo-Dobrovolsky D.V. and Krzhizhanovskaya M.G. (2017) Software for processing the X-ray powder diffraction data obtained from the curved image plate detector of Rigaku RAXIS Rapid II diffractometer. *Proceedings of the Russian Mineralogical Society*, **146**, 104–107.

Bruker-AXS (2014) *APEX2. Version 2014.11-0*. Madison, Wisconsin, USA.

Buerger M.J. (1954) The stuffed derivatives of the silica structures. *American Mineralogist*, **39**, 600–614.

Christidis P.C. and Rentzeperis P.J. (1976) The crystal structure of rhombohedral $Fe_2(SO_4)_3$. *Zeitschrift für Kristallographie – Crystalline Materials*, **144**, 341–352.

Dahmen T. and Gruehn R. (1993) Beiträge zum thermischen Verhalten von Sulfaten. IX. Einkristallstrukturverfeinerung der Metall(III)-sulfate $Cr_2(SO_4)_3$ und $Al_2(SO_4)_3$. *Zeitschrift für Kristallographie – Crystalline Materials*, **204**, 57–65.

Fedotov S.A. and Markhinin Y.K. (editors) (1983) *The Great Tolbachik Fissure Eruption*. Cambridge University Press, New York.

Hawthorne F.C., Krivovichev S.V. and Burns P.C. (2000) The crystal chemistry of sulfate minerals. Pp. 1–112 in: *Sulfate Minerals: Crystallography, Geochemistry, and Environmental Significance* (C.N. Alpers, J.L. Jambor and D. Nordstrom, editors). Reviews in Mineralogy & Geochemistry, **40**. Mineralogical Society of America and the Geochemical Society, Washington, DC.

Mandarino J.A. (1981) The Gladstone-Dale relationship. Part IV. The compatibility concept and its application. *The Canadian Mineralogist*, **14**, 498–502.

Nazarchuk E.V., Siidra O.I., Zaitsev A.N. and Vlasenko N.S. (2018) Koryakite, IMA 2018-013. CNMNC Newsletter No 43, June 2018, page 784; *Mineralogical Magazine*, **82**, 779–785.

Sheldrick G.M. (2015) Crystal structure refinement with SHELXL. *Acta Crystallographica*, **A71**, 3–8.

Slater P.R. and Greaves C. (1994) Powder neutron diffraction study of the Nasicon-related phases. $Na_xM^{II}_x\ M^{III}_{2-x}\ (SO_4)_{3-y}(SeO_4)_y$: $M^{II} = Mg$, $M^{III} =$ Fe, In. *Journal of Materials Chemistry*, **4**, 1469–1473.

Vergasova L.P. and Filatov S.K. (2012) New mineral species in products of fumarole activity of the Great Tolbachik Fissure Eruption. *Journal of Volcanology and Seismology*, **6**, 281–289.